Appl. Phys. A (2015) 118:1039–1042
DOI 10.1007/s00339-014-8866-5

Applied Physics A
Materials Science & Processing

Photoluminescence of CdTe nanocrystals grown by pulsed laser ablation on a template of Si nanoparticles

A. Guillén-Cervantes · H. Silva-López · M. Becerril-Silva · J. S. Arias-Cerón · E. Campos-González · A. C. Medina-Torres · O. Zelaya-Ángel

Received: 14 July 2014 / Accepted: 31 October 2014 / Published online: 12 November 2014

Abstract CdTe nanocrystals were grown on eroded Si (111) substrates at room temperature by pulsed laser ablation. Before growth, Si substrates were subjected to different erosion time in order to investigate the effect on the CdTe samples. The erosion process consists of exposition to a pulsed high-voltage electric arc. The surface consequence of the erosion process consists of Si nanoparticles which acted as a template for the growth of CdTe nanocrystals. CdTe samples were studied by X-ray diffraction (XRD), room temperature photoluminescence (RT PL) and high-resolution transmission electron microscopy (HRTEM). CdTe nanocrystals grew in the stable cubic phase, according to XRD spectra. A strong visible emission was detected in photoluminescence (PL) experiments. The PL signal was centered at 540 nm (∼2.34 eV). With the effective mass approximation, the size of the CdTe crystals was estimated around 3.5 nm. HRTEM images corroborated the physical characteristics of CdTe nanocrystals. These results could be useful for the development of CdTe optoelectronic devices.

1 Introduction

Since the discovery that nanocrystalline materials have interesting physical properties, these materials have found many applications. Recently, II–VI compounds synthesized at nanometric scale have been considered as building blocks [1, 2] to construct and design nanoscale photonic devices and sensors [3–9]. In the field of renewable energy it was estimated that with CdTe and CdS nanocrystals applied in the tailoring of solar conversion devices, the efficiency could increase considerably beyond the Shockley–Queisser limit in the near future [10]. The impact of CdTe synthesized at nanometric dimensions in biotechnology and health care sciences has been successfully proven with the development of optical chemosensors and biosensors [11–13]. In general, the potential applications of CdTe nanocrystals with controlled physical dimensions are unlimited, and this is the reason the study of their characteristics becomes important. On the other hand, the erosion by high-voltage electrical arc discharge is a simple low-cost method that modifies the electronic properties of semiconductor materials. The technique consists in applying a pulsed high voltage between a polarized needle, which works as anode, and a substrate biased as cathode [14, 15]. The morphology observed in the processed materials by this technique presents a number of holes and a large quantity of grains. The dimensions of the grains depend on experimental conditions involved in the process, such as: surrounding atmosphere, temperature, voltage, among others. For this work, Si nanoparticles produced on the eroded Si (111) surface were used as a template for the growth of CdTe nanocrystals. CdTe nanocrystals were deposited by pulsed laser ablation (PLA). The interest of this work was the development of CdTe nanocrystals on the well-established Si technology to promote the development of optoelectronic devices at nanometric scale.

2 Experiment

The (111) surface of Si substrates, doped with boron, with a resistivity of 0.01 ohm-cm were used in the experiments.

A. Guillén-Cervantes · H. Silva-López (✉) · M. Becerril-Silva · J. S. Arias-Cerón · E. Campos-González · O. Zelaya-Ángel
Physics Department, CINVESTAV-IPN, Apdo. Postal 14-740, 07360 Mexico, Mexico
e-mail: hsl@fis.cinvestav.mx

A. C. Medina-Torres
Escuela Superior de Física y Matemáticas del IPN, 07738 Mexico, Mexico

The Si (111) substrates were chemically cleaned in HF before the erosion process. The substrates were subjected to erosion with a pulsed power supply working at 12 kV and a frequency of 11 kHz. The positive high-voltage terminal was applied to a tungsten wire whose tip was separated 1 mm from the Si substrates which were connected to the negative terminal of the power supply. The erosion of the samples was performed in air, at room temperature varying the erosion time from 3 to 30 min. After this process, eroded Si (111) substrates were loaded into the pulsed laser ablation chamber. High purity (99.99 %) CdTe powders were employed to form the target. Depositions were carried out at room temperature under an Ar atmosphere. The pressure in the deposition chamber during growth was 10^{-4} T. Films were deposited with a Nd:Yag laser at 1,064 nm using a pulse width of 5 ns and repetition rate of 10 Hz with a laser fluence of 2 J/cm^2. The separation between the target material and the substrates was 2 cm. The growth time was 5 min; with these conditions, CdTe films of 1 μm are grown on the conventional substrates. The crystalline structure of the films was determined by X-ray diffraction (XRD) in a Siemens D-5,000 equipment with the Cu–Kα line with a wavelength of 1.5406 Å. For the RT PL measurements, an Omnichrome He–Cd laser with the 325 nm line and optical excitation power of 15 mW was employed at room temperature. The emission signal was focalized to the entrance of a Jobin–Yvon HRD-100 monochromator and detected with an Ag–Cs–O Hamamatsu photomultiplier. High-resolution transmission electron images were performed in a Jeol 2010 microscope at 200 kV. CdTe specimens were detached from the films and attached to standard copper grids to image the nanoparticles.

3 Results and discussion

The XRD patterns of CdTe films grown on Si (111) substrates by PLA deposition are displayed in Fig. 1. Before growth, Si (111) substrates were eroded with an electric arc discharge at different time indicated in the figure. In general, the spectra present signals at 23.68°, 39.26° and 46.42°. These signals were assigned to the (111), (220) and (311) planes, respectively, of CdTe in cubic phase [16, 17]. An additional feature appeared in the spectra; the peak centered at 28.36° corresponds to a reflection of Si (111) due to the substrate (ICDD Data Card 00-001-0787).

The predominant intensity of the (111) planes suggests samples grew with preferential orientation. From the peaks position and with the following formula [18]:

$$d = \frac{n\lambda}{2\sin\theta}$$

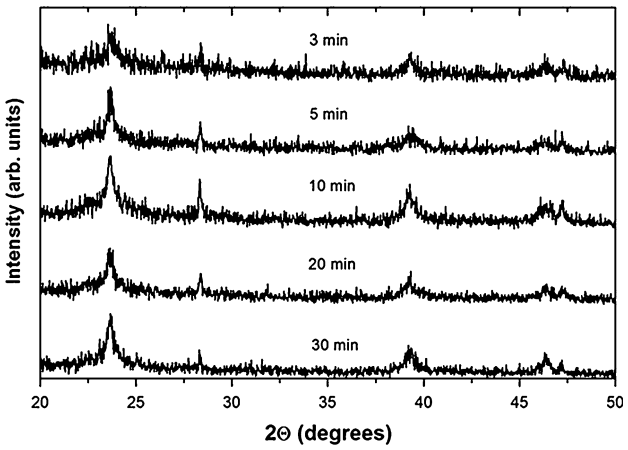

Fig. 1 XRD patterms of CdTe nanocrystals grown by laser ablation on eroded Si (111) substrates. *Note* the CdTe signals correspond to cubic phase

Table 1 Interplanar distance of the different planes of the CdTe nanoparticles

CdTe plane	Estimated interplanar distance (Å)
(111)	3.75
(220)	2.29
(311)	1.95

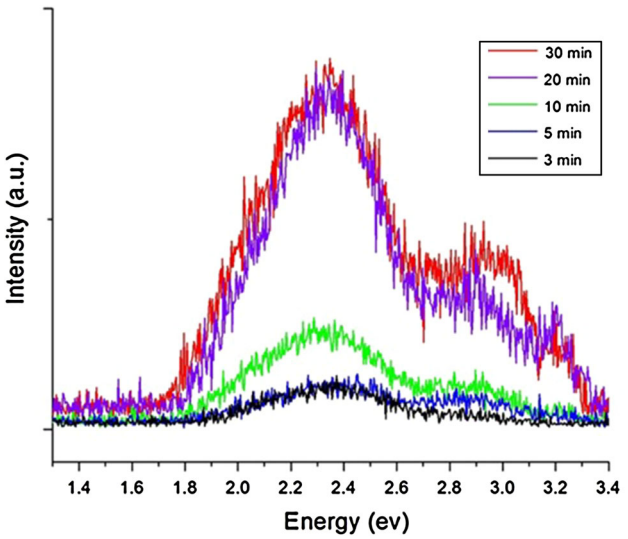

Fig. 2 RT PL of CdTe nanocrystals deposited on eroded Si substrates. An intense signal centered at 540 nm (2.3 eV) can be distinguished and is due to CdTe nanocrystals. A shoulder peaked at 2.91 eV can be ascribed to Si nanoparticles

where n is the order of the reflection, λ is the wavelength of the X-ray source, θ is the angle and d refers to interplanar distance, the interplanar distance for the different planes was evaluated; results are summarized in Table 1. The lattice

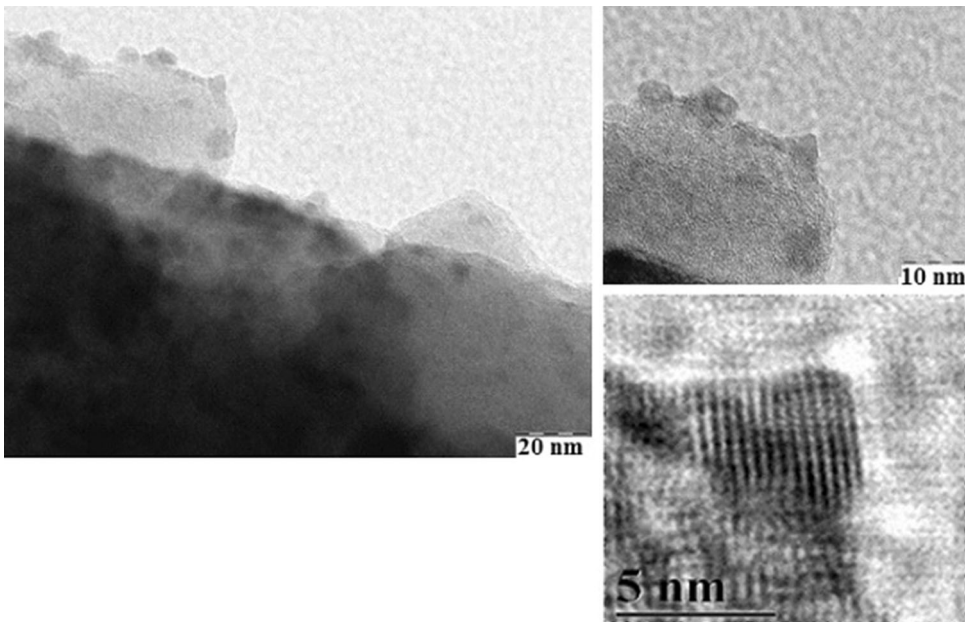

Fig. 3 TEM image of CdTe nanocrystals grown on a Si substrate by pulsed laser ablation deposition

constant a calculated was 6.49 Å, and this result is consistent with the reported values [19], for CdTe in cubic phase.

The RT PL spectra of the CdTe nanoparticles deposited by PLA on eroded Si (111) substrates are depicted in Fig. 2. In the spectra, a broad signal centered at 540 nm (2.34 eV) can be observed.

The RT PL intensity of this signal increases as a function of the erosion time in the substrates. From the figure, note that CdTe samples grown on Si substrates with less erosion time show a weaker intensity in the RT PL emission, and this is the case for samples with 3, 5 and 10 min. Samples deposited on those substrates with 20 and 30 min of exposition to the electric arc present the most intense RT PL signal. In the spectra, another feature detected at 440 nm (2.91 eV) was assigned to porous Si [20]. From the RT PL spectra and with the effective mass approximation [21],

$$E(D) = E_g + \frac{2\pi^2\hbar^2}{D}\left[\frac{1}{m_e^*} + \frac{1}{m_h^*}\right] - \frac{3.572e^2}{\epsilon D}$$

the size of the nanoparticles was calculated, where $E(D)$ is the center energy of the emission band, E_g is the bulk CdTe band gap considered as 1.49 eV, m_e^* and m_h^* are the effective mass of the CdTe electrons and holes, respectively, ε is the CdTe dielectric constant and, finally, D is the diameter of the nanoparticles. The calculated value was 3.5 nm, and our results show agreement with those reported previously [22–26].

An important remark should be mentioned considering the RT PL spectra shown in Fig. 2, the emission centered at 540 nm (2.3 eV) associated to CdTe nanocrystals does not shift in spite the difference in erosion time substrates were subjected to, besides, the intensity, as aforementioned, increases as a function of the erosion time. This fact indicates that nanoparticles are generated immediately since the early stages of the erosion process and suggests also that when the erosion time increases the number of nanoparticles increases drastically on the surface of the Si substrates. The Si nanoparticles, consequence of the erosion process, acted as a template for the synthesis of CdTe nanocrystals deposited by PLA. The result is a strong increase in the RT PL signal. Even at reduced erosion times, nanoparticles with the same distribution in size can be produced with the electric arc erosion process. The experiments reported in this work represent a low-cost process to produce nanoparticles on Si substrates and compatible with most of the techniques to grow II–VI materials.

Figure 3 is a HRTEM image of the CdTe nanocrystals deposited by PLA on eroded Si substrates. The image shows the physical dimensions and morphology of the nanoparticles, note the spherical shape, according to the scale the nanoparticles have around 4 nm in diameter. The dimensions coincide with the calculated size estimated from XRD and RT PL analyses. An image of the crystalline structure of the CdTe nanocrystals is presented in Fig. 3. From this HRTEM image, the interplanar lattice distance was evaluated in 3.7 Å a value in agreement with that reported in literature for the (111) planes in CdTe [27].

4 Conclusions

CdTe nanocrystals were deposited by PLA on Si (111) eroded substrates. Before growth, Si substrates were

subjected to a high-voltage electric arc to produce nanograins. Si nanograins acted as a template for the growth of CdTe nanocrystals. Results showed a strong RT PL emission on samples grown on substrates exposed for 20 and 30 min to erosion process. The RT PL signal in the visible region centered at 540 nm. These samples are potentially useful for the development of light emission devices tailored on Si technology.

Acknowledgments The authors acknowledge the technical support of Marcela Guerrero from CINVESTAV-IPN and the partial support by CONACyT-México.

References

1. J.-J. Shi, S. Wang, T.-T. He, E.S. Abdel-Halim, J.J. Zhu, Ultrason. Sonochem. **21**, 493 (2014)
2. V. Lesnyak, A. Wolf, A. Dubavik, L. Borchardt, S.V. Voitekhovich, N. Gaponik, S. Kaskel, A. Eychmüller, J. Am. Chem. Soc. **133**, 13413 (2011)
3. C. Burda, X. Chen, R. Narayanan, M.A. El-Sayed, Chem. Rev. **105**, 1025 (2005)
4. A. Ruland, C. Schulz-Drost, V. Sgobba, D.M. Guldi, Adv. Mater. **23**, 4573 (2011)
5. D.V. Talapin, J.-S. Lee, M.V. Kovalenko, E.V. Shevchenko, Chem. Rev. **110**, 389 (2010)
6. I. Gur, N.A. Fromer, M.L. Geier, A.P. Alivisatos, Science **310**, 462 (2005)
7. R. Gui, X. An, H. Su, W. Shen, Z. Chen, X. Wang, Talanta **94**, 257 (2012)
8. L. Zhu, L. Xu, J. Wang, S. Yang, C.-F. Wang, L. Chen, S. Chen, RSC Adv. **2**, 9005 (2012)
9. L.E.S. Rohwer, J.E. Martin, X. Cai, D.F. Kelley, ECS J. Solid State Sci. Technol. **2**(2), R3112 (2013)
10. J. Wang, I. Mora-Seró, Z. Pan, K. Zhao, H. Zhang, Y. Feng, G. Yang, X. Zhong, J. Bisquert, J. Am. Chem. Soc. **135**, 15913 (2013)
11. T. Asefa, C.T. Duncanc, K.K. Sharma, Analyst **134**, 1980 (2009)
12. H. Wang, L. Sun, Y. Li, X. Fei, M. Sun, C. Zhang, Y. Li, Q. Yang, Langmuir **27**, 11609 (2011)
13. N.T.K. Thanh, L.A.W. Green, Nano Today **5**, 213 (2010)
14. R.E. Hummel, S.-S. Chang, Appl. Phys. Lett. **61**, 1965 (1992)
15. V.A. Vons, L.C.P.M. de Smet, D. Munao, A. Evirgen, E.M. Kelder, A. Schmidt-Ott, J. Nanopart. Res. **13**, 4867 (2011)
16. X. Wang, J. Wang, M. Zhou, H. Zhu, H. Wang, X. Cui, X. Xiao, Q. Li, J. Phys. Chem. C **113**, 16951 (2009)
17. M.H. Ehsani, H.R. Dizaji, S. Azizi, S.F.G. Mirmahalle, F.H. Siyanaki, Phys. Scr. **88**, 025602 (2013)
18. B.D. Cullity, *Elements of X-ray diffraction.* Addison Wesley Mass. (1978)
19. V.V. Ison, A.R. Rao, V. Dutta, Sol. Energy Mater. Sol. Cells **93**, 1507 (2009)
20. N.A. Piskunov, E.D. Maslennikov, L.A. Golovan, P.K. Kashkarov, I.A. Ostapenko, S. Rodt, D. Bimberg, Laser Phys. **21**, 614 (2011)
21. M.H. Ludwig, R.E. Hummel, M. Stora, Thin Solid Films **255**, 103 (1994)
22. J. Kolny-Olesiak, V. Kloper, R. Osovsky, A. Sashchiuk, E. Lifshitz, Surf. Sci. **601**, 2667 (2007)
23. H. Zhong, M. Nagy, M. Jones, G.D. Scholes, J. Phys. Chem. C **113**, 10465 (2009)
24. W.W. Yu, L. Qu, W. Guo, X. Peng, Chem. Mater. **15**, 2854 (2003)
25. J. Guo, W. Yang, C. Wang, J. Phys. Chem. B **109**, 17467 (2005)
26. H.-B. Bu, H. Kikunaga, K. Shimura, K. Takahasi, T. Taniguchi, D.G. Kim, Phys. Chem. Chem. Phys. **15**, 2903 (2013)
27. X.-Y. Lv, W.-J. Chen, J.-W. Hou, Z.-H. Jia, F.-R. Zhong, T. Jiang, Mater. Sci. Forum **663**, 64 (2011)